On the processing of steel rod for agricultural conveyor systems

Turner, Richard; Perumal, Bama; Thota, Bhaskar; Brooks, Jeffery

DOI:
10.1016/j.jmapro.2017.01.005

On the processing of steel rod for agricultural conveyor systems: Materials characterisation and modelling

R.P. Turner, B. Perumal, B. Thota, J.W. Brooks

PRISM[2] Research Group, School of Metallurgy & Materials, University of Birmingham, Birmingham, B15 2TT, UK

Abstract

A supply of medium carbon boron steel rod has been used industrially to produce the "rib-like" rod structures for mechanical conveyor systems, used across a number of non-safety critical industries, such as agricultural harvesting. The steel rod is resistive-heated and subsequently mechanically deformed such to produce a small region of flattened proportions, to allow for easier mechanical attachment to a belt system to attach all rods to the conveyor system. It has been noted industrially that after the flattening operations have taken place, a region at the shoulder of the flattened section is susceptible to cracking problems. The root cause of this cracking was desired to be understood, hence three likely causations for the cracking were explored, namely (i) mechanical stresses at the region, (ii) micro-segregation of the alloying elements at the location, and (iii) overheating. A 2D axi-symmetric finite element framework was developed to predict the stresses generated in the flattened section. This model showed that there were some areas of concern regarding the predicted effective stress and strain distributions, compared to the material flow stresses, thus potentially a mechanical reason for the cracking to occur. Microscopy methods were considered to understand the microstructure of the surrounding material and the nature of the cracks. However, these suggested that there was no likely element segregation to cause a significant variation in material property. Finally, temperatures generated by the resistive heating procedure were measured, and this does suggest that the material may have been overheated, thus producing coarser austenite grains whilst the material is held at elevated temperatures for a short time, and so producing inferior mechanical properties in this small region of heated material. The effects of overheating are impossible to eliminate without a complete re-melt of the steel. Thus, the research has demonstrated that a combination of overheating, and in-situ stress and strain distributions, could be the root cause of the cracking.

Keywords: finite element, microstructure, thermal, ferrite, grain boundary, precipitate.

1. Introduction

The use of approximately 8-15 mm diameter steel round rod within predominantly non-safety critical mechanical conveyor systems to transport produce is relatively commonplace [1]. Thus, component non-conformance and "defect-tolerances" are admissible up to certain levels within the steel rods. Conveyor systems are widely used in a number of industries, including agricultural harvesting [1], whereby the produce can be transported from the lifted earth to a container attached to the harvesting vehicle, by means of a rigid conveyor system typically manufactured from alloyed steel rods, processed such that they can be joined using heavy-duty reinforced rubber or woven fabric to form a conveyor-system.

The medium carbon boron steel rods used in this work contained nominally 0.003 wt% boron. The addition of 0.0008 – 0.005 wt% boron to the steel is understood from the literature to significantly increase yield strength and UTS, improve the elongation of the steel, improve the impact toughness and enhance martensite formation [2]. Boron steels are also renowned for their high hardenability, thus are suitable for use in the production of rods which are to be used in both hot and cold forming operations and production of bolts or other rigid structures [3]. The boron acts as a grain refining addition to the alloyed steel, and upon quenching and/or tempering produces the finer grain structure which provides a more uniform material property across the finished part.

Medium carbon boron steel rod is commonly processed such that pieces of the rod of desired length are formed with flattened panel sections with a larger flat surface area than the remainder of the round rod (see Figure 1a). This allows for holes to be introduced through the flattened sections, providing a mechanical fixture route to the conveyor's rubber belt system. Typically a flattened section would be formed at a central region, and at either end of the rod to allow for mechanical attachment of each rod at each location to the conveyor belt drive band (see Figure 1b) with reinforced flattened sections about the centre which are subject to additional processes, as described below, prior to attachment to the central drive band.

The formation of the reinforced flattened section about the centre is performed in typically a number of operations, ideally linked together as a continuous processing route. Firstly, the section of rod to be flattened is heated using a suitable heating method. For speed, resistive heating is often employed. The rod, heated up to in excess of an estimated 1100 °C in this area, is then upset closed-die forged by a small amount. Clearly the flow stresses of the heated region are far lower than those of the cold remainder of the rod, hence all the distortion observed arises in the heated region of the rod, as it upsets into the closed die shape. This produces an intermediate rod product with a bulged section in all radial directions, at the relevant location on the rod where the flattened region is required. A subsequent operation is then performed to press this bulged region down to form something that is flattened, breaking the axi-symmetric condition of the rod which had been preserved until now, leaving the final flattened part which is less high than the rest of the rod, but considerably wider. Further processing operations see holes introduced through the flat area for mechanical attachment purposes (see Figure 2).

During the processing operations, the steel is subjected to severe thermal and mechanical conditions. After the final flattening processing operation that the rod experiences, small cracks can occasionally be observed. These cracks typically occur in the shoulder area of the flattened section (see figure 3a). It therefore becomes of great interest to understand the driving mechanism for the cracking of the steel rod in these locations. It is considered that the cracking could have arisen due to a number of reasons: (a) Mechanically the rod has been subjected to stresses and strains from the forming presses that have exceeded the load-bearing capability, and the rod has as result suffered cracking damage, (b) Thermally the rod has been overheated, which has caused sulphur inclusions to be present at or close to grain boundaries, (c) The steel rod has suffered from element segregation which has significantly changed the properties of the material in highly localised areas, which has allowed for the cracking to occur in such a region. In order to assess why the steel rod has cracked at the location noted, experimental analysis using finite element modelling (for stress analysis), Scanning-electron microscopy (SEM) and optical microscopy (for microstructure variations) and infra-red thermal measurements (for temperature assessments) were taken.

2. Methodology

2.1 Experimental Procedures

2.1.1 Material composition

The material used in the study was medium carbon boron steel, rolled to a 12mm diameter rod. Nominal composition of this steel is given in table 1. Rod was purchased from a number of different suppliers, and chemical analysis of different suppliers' rod showed that, although always within tolerance, the composition of the rod could vary with some considerable amounts. Notably, the manganese content could vary from 1.0 – 1.4 wt%, boron could vary from 0.003 – 0.005 wt%, and sulphur could vary from 0.005 - 0.02 wt%.

2.1.2 Metallographic preparation

The microstructural evolution of material in as-received condition and in the thermo-mechanically deformed condition was studied using the ZEISS Axioskop2 Light Optical Microscopy (LOM) facility available in the School of Metallurgy & Materials at the University of Birmingham, using a standard metallographic preparation method [4]. The as-received and upset forged steel rod samples have been sectioned. The sectioned steel rod specimens were mounted under pressure using conductive Bakelite powder. After mounting the specimens, the grinding preparation was performed with silicon carbide (SiC) papers with a range of grit sizes incrementally moving from the coarse 240 grit paper to the fine 1200 grit paper. After the grinding steps, these specimens were polished by Struers MD Largo disk, using Diamond paste suspensions of 9µm, 3µm, and 1µm abrasive material during polishing. These samples were subsequently etched using a solution of Kalling's etchant (consisting of 0.5ml Copper Chloride, 100ml Hydrochloric acid and 100ml Ethanol) for about 30 seconds to reveal the microstructure.

2.1.3 As-received and heated material microstructure

The as-received microstructure of the steel rod shown in figure 3a consists of ferrite grains in the grain boundaries of the acicular pearlite grains. The microstructural evolution of mechanically deformed steel rod sample was examined along the longitudinal and transverse directions on the sample surface (see figure 3b) subsequently closer to edges and cracks to understand the change in microstructure and driving mechanism for the cracking on the deformed sample. In this work, Scanning Electron Microscope (SEM) imaging was undertaken using a Philips XL-30 SEM, at the School of Metallurgy and Materials, University of Birmingham. The SEM images, along with optical imaging are considered to be the efficient tool to detect the intergranular fracture surface and the facets (precipitates) on the grain boundaries, on the overheated fracture surfaces.

2.2 Finite Element Modelling

In order to assess the mechanical loading upon the steel rod as it undergoes the forming processes, finite element (FE) methods have been employed to simulate the process. The FE software selected to perform the modelling of the heating and forging stages of the operation was the general, multi-purpose [5] FE software Deform (v11.0.2). A 2D axi-symmetric model was built to replicate the heating and subsequent deformation process on the specimen. A section of rod 300 mm in length was considered appropriate for modelling. The width of the rod in the model is 6mm, as it is an axi-symmetric model and as such with the axis of symmetry down the centre-line of the rod, so the model is appropriate for a 12mm diameter rod. A graded mesh, with finer elements (of ~0.25mm in length) at the region to be heated and deformed by the forging operations, coarsening out away from the heated region (to elements of approximately 4mm in length), was chosen. A graded mesh as such is standard within FE modelling methods to reduce the model simulation time by reducing complexity at areas of very low thermal and deformation gradients. The medium carbon boron steel was approximated as a material file containing tabular temperature dependent Young's Modulus, Poisson ratio, density, thermal conductivity, specific heat and thermal expansion coefficient, and containing tabular data for the material flow stress, as a function of temperature and strain rate, using the materials modelling software JMatPro [6]. The materials data is considered from very low strain rates (10^{-3} s^{-1}) to high strain rates (10^3 s^{-1}). However for this process a low strain rate is applicable. Similarly, the material data is entered from room temperature up to the resistive heating temperature of 1200 °C.

The heating of the rod through resistive heating methods was simulated by considering a short thermal calculation of a few seconds timeframe, representative of the actual resistive heating process. In this section of modelling, there is no deformation considered, and the estimated resistive heating parameters are entered in to the model and considering the geometry of the rod. Due to the age of the equipment, the resistive heating process is rather unrepeatable; hence this must be considered a simplification, and a possible source of modelling errors. The heated rod was then transferred to a different modelling set-up, with the geometry of the tooling used in the closed-die forging operation included. Experimental measurements of the force applied by the tooling suggested that the force used was approximately 50 kN. As such, in the finite element model a 50 kN force was applied to one end of the rod, whilst the other end was considered to be clamped against a fixed wall. The set-up of the modelling operations in FE software Deform can be seen in Figure 7a.

2.3 Thermal Measurements

The rod heating process is undertaken using resistive heating methods. Resistive heating is a process whereby an electric current is passed through a conductive material (such as the steel rod in this work) from one junction to another. The resistive heating unit in this work placed two junctions on to the surface of the medium carbon boron steel rod, at a separation distance of approximately 130mm. Thermal measurements of the surface of the heated region of rod were taken using a Thermosense HL-1600 Infra-red thermometer. This equipment has a response time of less than 1 second and accuracies of +/- 5% in the worst cases. At the temperatures indicated by the infra-red thermometer in this particular use, the typical error should be limited to +/- 3.5%, although for conservatism the 5% margin of error has been considered with the data.

The infra-red thermometer was used to conduct two experimental measurements. Firstly, to measure the temporal evolution of the peak surface temperature of the heated steel rod as it came off the resistive heater. An initial delay of approximately 2seconds was observed as the rod was moved, thus the initial temperature measurement was considered at 2 seconds. Further measurements were taken at initially 2 seconds intervals (up to 10 s), coarsening to 5 second intervals (up to 30 s), 15 second intervals (up to 90 s), and latter measurements taken at 120 and 180 seconds. The infra-red thermometer was switched to its so-called "max" mode, and the IR gun directed in front of the rod, pointing at the heated section, from a distance of ~100mm away. Secondly, for repeatability of the resistive heating process, two measurements of the thermal profiles of resistive heated bars as it came off the resistive heating unit, across the length of the bar, were made.

3. Results

3.1 Microscopy Analysis

This work has been carried to study the microstructural evolution of medium carbon boron steel rod which was heated and then mechanically deformed at temperatures exceeding 1100 °C. Most of the defects in the heated steels are attributed to faulty procedure such as overheating, "burning" and non-uniform heating and quenching. However, simple visual examination of these parts doesn't recognize the defects of overheating, "burning" and residual stress development in steels. When steel is heated above 1100 °C working temperature, changes take place at the austenitic grain boundaries which in turn reduce the fracture resistive of the steel in that region and this causes deterioration in the room temperature mechanical properties after hot working [7]. After being held at elevated temperature, steels usually develop the grain boundary facets in an overheated area. The size and number of facets increase with increasing temperature. On the other hand "burning", similar to overheating; occurring due to an elevated temperature usually in excess of 1100 °C develops the strings of sulphide inclusions along the grain boundaries. The term "burning" can occur at a temperature below the solidus of an alloy but free from the sulphur present in the alloy [8].

The key objective of the work is to understand the root cause for the fracture that occurred in the shoulder area and the immediate location of the flattened section of the steel rod used in the conveyor systems – Figure 3a shows the optical microscopy and SEM images of the as-received medium carbon boron steel. It therefore becomes of considerable interest to link the fracture surface back to microstructural data. To attempt to make this link between cause of fracture and microstructure, the following evidence is analysed.

The initial microstructure examination of the observed cracking, using both an optical and SEM microscopy approach, is presented in Figure 4. The optical and SEM images of the given medium carbon boron steel rod in Figure 4 revealed that the fracture mode was intergranular ductile fracture. A number of micro-void cracks are evident from the optical microscopy and SEM images ahead of the main macroscopic crack of concern. After etching of the steel rods, the original austenite grain boundaries are attacked by the etchant which preferentially affected the matrix and leaving the grain boundaries unaffected which appears as a white network as shown in Figures 5 and 6.

Further microstructure analysis was performed along the longitudinal and transverse directions (indicated in Figure 3b), both at locations close to the crack surface on the steel rod, and further away from the crack. Optical microscopy images in Figure 5 show that there is a significant increase in the grain size of austenite as compared to the un-heated as-received microstructure (see Figure 3a) of the parent medium carbon boron steel.

During high temperature heating the sulphide inclusions are dissolved, and with subsequent cooling below the overheating temperature the sulphur inclusions will precipitate along the grain boundaries. The presence of sulphides on the grain boundaries, as shown in Figure 6, provides a preferential, low energy fracture path which may lead to a ductile intergranular fracture. Intergranular fracture occurs when there is reduction of cohesion along the grain boundaries. In steels the presence of precipitates and residual impurities are harmful in lowering the cohesion along the grain boundaries. Embrittlement increases when impurities react with elements such as Mn and Cr [9]. The precipitates along grain boundaries are observed both close to the crack tip and at a location well away from the crack (but still in the overheated region). This illustrates that the problematic region of bar is widespread, and not a highly localised phenomena.

It is also understood that if there is a possibility for the intergranular/intercrystalline ductile fracture, etching tends to progress preferentially along the grain boundaries which results from the difference in composition of the alloy and grain boundary. The work of McLeod and Nutting [10] and Funnell [11] suggested methods to avoid the precipitates of MnS and AlN and control/decrease the amount of sulphur and aluminium content to avoid the microstructural changes which leads to embrittlement during heat treatment of steel, have been often reported in the literature [12-15]. In addition to the precipitate, the grain boundaries are further weakened by the exposed high temperatures, where the most predominant fracture path becomes intergranular fracture [16].

3.2 Finite Element Modelling

The finite element (FE) modelling work focused upon the heating and the initial axial shortening operation within the overall component process. Firstly, the heating model was set-up using the peak temperature measured experimentally when the rod is taken off the resistive heater to be placed on to the axial forging rig (see Fig 7a). The finite element predictions for the distribution of temperature are shown in Figure 7b. In order to validate the FE model thermal predictions, approximate measurements were taken of the heated region of rod experimentally, using the infra-red thermometer moving axially along the rod, to record the temperature variation.

Whilst it is accepted that the time taken to take each measurement and move to the next location on the rod will have allowed the rod to additionally cool (thus strictly the experiment is not capturing a snap-shot in time of the rod), given the air-cooling process produces a relatively slow heat transfer, this was accepted as a simplification to the experiment. Comparisons of the two experimentally measured thermal profiles critically compared to the FE model is given in Figure 8. The difference in the experimental measurements highlights the degree of unrepeatability within the resistive heating process. However, it is considered that the agreement between the FE predictions and the measured thermal data is shown to be reasonable, thus offering some assurance that the FE model is considering the correct thermo-physical processes occurring in the real process, and offering a sensible validation to the thermal modelling.

The applied force from the piston on the rig was measured, and entered appropriately to the next stage of the FE model, simulating the coupled thermo-mechanical deformation of the rod on the axial forging rig. The FE model predicted strain and stress distributions occurring within the steel rod are shown in Figure 9a and 9b respectively. The peak effective stress observed within the rod at the location where cracking is observed is predicted to be of approximately 600MPa tensile stress. The temperature of the rod at this location, at the instant that the effective stress peaked, was in the region of 530 – 560 °C.

Consulting the flow stress data from materials modelling software JMatPro for this steel, for the combination of temperature (approximately 530-560 °C) and strain (approximately 0.85), then depending upon strain rate, the flow stress of the material would be of the order of 650 MPa to 920MPa. At the lower strain rates (10^{-3}~$10^{-2}s^{-1}$) that are likely in this process, the corresponding material flow stresses of 650 – 710 MPa exceed the predicted effective stress experienced by the processing route. However, given the very close proximity of the values of flow stress of the rod compared to the FE predicted effective stress, if the analyst takes necessary experimental and modelling errors into consideration, the FE model suggests that the stresses and strains experienced at the shoulder region does indicate a potential problem with cracking and damage at this location, although it is by no means a certainty that cracking would be expected in the process.

3.3 Thermal Measurements

The temperature on the surface of the heated rod was recorded using the infra-red thermometer described. In this experiment, the heated rod was left to air-cool without any external tooling or loading in contact with the rod. The thermal history of the heated region of rod can be seen in

Figure 10. By linear regression methods using the thermal readings at 2, 4, 6, 8 and 10 seconds, we can estimate that the actual peak temperature achieved during resistive heating was at least 1175 °C, and possibly even hotter than 1200 °C when the relative errors of the measurement are taken in to consideration. The fact that the experimental measurements suggest that the medium carbon boron steel will have exceeded the 1100-1200 °C range could be critical, given that overheating of steels is often considered to be the time that the object is exposed to temperatures in excess of 1100 °C [7, 17], and this effect is exacerbated by the increased peak temperatures up toward 1200 °C.

Thus, the elevated temperature that is achieved with the resistive heating of the rod can lead to overheating of the steel at this location. Microstructural changes will take place at the austenitic grain boundaries [15], which reduce the material resistive to fracture. These microstructural changes cannot be rectified with a heat treatment process. The effects of overheating/"burning" are impossible to eliminate without a complete re-melt of the steel. However, for the rod considered in this analysis, it must be noted that the rod had not yet been subjected to the post-processing heat-treatment operations appropriate for the industrial application.

Additionally, it must be noted that as the process is taking place in an oxygen atmosphere, and as such an oxidised surface will be formed, the infra-red thermometer as a line-of-sight measurement method will therefore record the temperature of the oxidised material at the surface. The oxidised material may have a different conductivity and emissivity value, hence some pragmatism must be adopted when analysing infra-red thermal data.

Unfortunately, the resistive heating equipment used was very old, and as such manual controlling of the process is very limited. If improvements were to be sought for this process of resistive heating, then through-process thermal monitoring as standard would be needed, and the system automatically shutting off when the rod surface temperature reaches approximately 1100 °C, hot enough to allow for the rod deformation with the applied force, but not so hot as to lead to overheating.

4. Summary & Conclusions

Evidence of severe cracking damage had been observed within the shoulder regions of the formed flattened sections of the medium carbon boron steel, after processing. A number of experimental methods were considered to determine the reasons for the steel rod to suffer such issues during the component production. The following conclusions were drawn:

- There is some evidence from finite element (FE) modelling that the steel rod at this critical shoulder region, during the processing, may experience levels of stress or strain that would raise concerns regarding material suffering damage. However, this is based upon certain assumptions and taking in to account a certain margin of error within the mechanical predictions for the FE model.
- The microstructure images captured along the crack region showed that there is a significant change in the grain size on the mechanically deformed steel due to overheating/ burning. The grain size of initial as-received steel was 25 micron which was coarsening during hot working and increased in size to 60 micron. There is evidence that an increase in the rod temperature will lead to coarsening of austenite grains and after cooling this will show an increased amount of precipitate along the grain boundaries which will coarsen on further cooling and lead to intergranular fracture and the root cause for the cracks to develop along the austenite grain boundaries.
- The above experimental evidence supports that overheating / "burning" of medium carbon boron steel can increase the amount of precipitate on the austenite grain boundaries due to presence of sulphur content of about 0.02% and the manganese content of about 1.4%. It can be prevented by reducing the manganese content in the steel rod. However, whilst the addition of the boron as an alloying element helps to produce the finer grain structure, it appears to offer no improvement in the issue of steel overheating.
- Infra-red thermal measurements taken on the same operating equipment as used for the sample which displayed the cracking issues has shown resistive heating produces temperatures in the rod exceeding 1150 °C, and possibly exceeding 1200 °C. The temperature reached is significant, and consistent with evidence that the rod has been "burnt". Although as this is a surface measurement using line-of-sight, so any oxidised material will become the field of view.

5. Acknowledgements

The research carried out for this project was performed under the financial support of two ERDF-funded projects, namely the Accelerating Business-knowledge Innovation Activity (ABIA) project and the CHART (Materials Characterisation facility) project, both University of Birmingham led projects with the aim of supporting small-medium enterprise industries in the local area. Thanks are also offered to the industrial contacts for this piece of work - further details can be supplied by contacting the author if desired - for the advice offered on manufacturing routes, use of industrial equipment and the recording of thermal measurements. Additional thanks to Sente Software Ltd, Surrey, UK for the assistance with the material file for the medium carbon boron steel.

References

1. D.R. Heldman, *Encyclopedia of Agricultural, Food and Biological Engineering*, Marcel Dekker Inc, New York, 2003.
2. S.N. Ghali, H.S. El-Faramawy, M.M. Eissa, *J. Minerals and Mat Characterisation and Eng*. 11; pp995-999 (2012)
3. United States Steel International – Carbon and Alloy Steel Hot Rolled Wire Rods Selection Guide, ADUSS 50-7708-01, USA (1980).
4. D.C. Zipperian, Metallographic Specimen Preparation Basics, Pace Technologies, (www.metallographic.com/Technical/Basics.pdf) 2016.
5. Scientific Forming Technologies Corp., 2545 Farmers Drive, Columbus, Ohio 43235
6. Sente Software Ltd. Surrey Technology Centre, 40 Occam Road, GU2 7YG, United Kingdom.
7. A.K. Sinha, Defects and distortion in heat-treated parts, *ASM Handbook, Vol4*, Heat Treating, Bohn Piston division, pp. 601-619
8. A. Stansfield, The burning and overheating of steel, *Journal of the Iron and Steel Institute.* (London), 1903, Vol. 64, pp. 433-168.
9. C.J. McMahon, Intergranular Fracture in Steels, *Materials Science and Engineering*, 25 (1976) 233 - 239 233.
10. N. P. McLeod and J. Nutting: *Met. Technol.,* 1982, 9, pp. 399.
11. G. D. Funnell, in *'Hot working and forming processes'*, 104; 1979, London, The Metals Society.
12. G. D. Joy and J. Nutting: in 'Effect of second-phase particles on the mechanical properties of steel', *Journal of the Iron and Steel Institute*. 95; 1971, London.
13. R. N. O'Brien, D. H. Jack, J. Nutting: in *'Heat treatment '76'*, 161; (1976), London, The Metals Society.
14. T. Gladman and F. B. Pickering: *Journal of the Iron and Steel Institute*, (1967), 205, pp. 653
15. B. C. Woodfine and A. G. Quarrell: *Journal of the Iron and Steel Institute,* (1960),195, 409.
16. S. Lampman, Intergranular Fracture: *ASM Handbook - Failure Analysis and Prevention* (ASM International) 2002, pages 641-649.
17. K. Tsun, The Overheating & Burning of Steel. *Symposium on Industrial Failure of Engineering Metals & Alloys*, Feb. 5-7 (National Metallurgical Laboratory, Jamshedpur) (1953).

Figures & Tables

Table 1: Nominal chemical composition of the medium carbon boron steel rod.

	C	**Si**	**Mn**	**P**	**S**	**Ni**	**Cr**	**Mo**	**Cu**	**N**	**Al**	**Ti**	**B**	**Fe**
Chemical composition	**0.34**	**0.19**	**1.4**	**0.01**	**0.02**	**0.09**	**0.35**	**0.03**	**0.18**	**0.01**	**0.025**	**0.05**	**0.003**	**Rem**

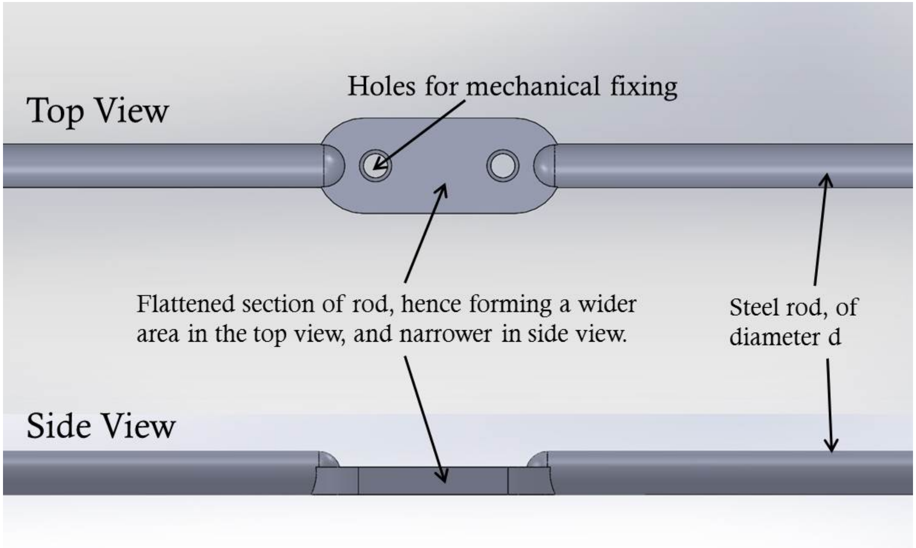

Figure 1a: *Schematic of the forming of a flattened section for mechanical attachment purposes.*

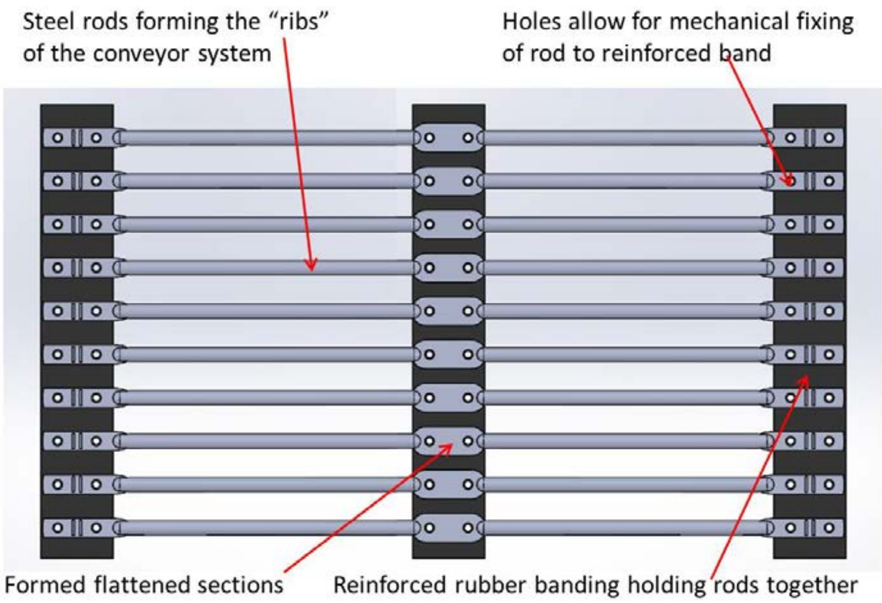

Figure 1b: *Schematic of the constructed conveyor system from processed steel rods with a flattened section*

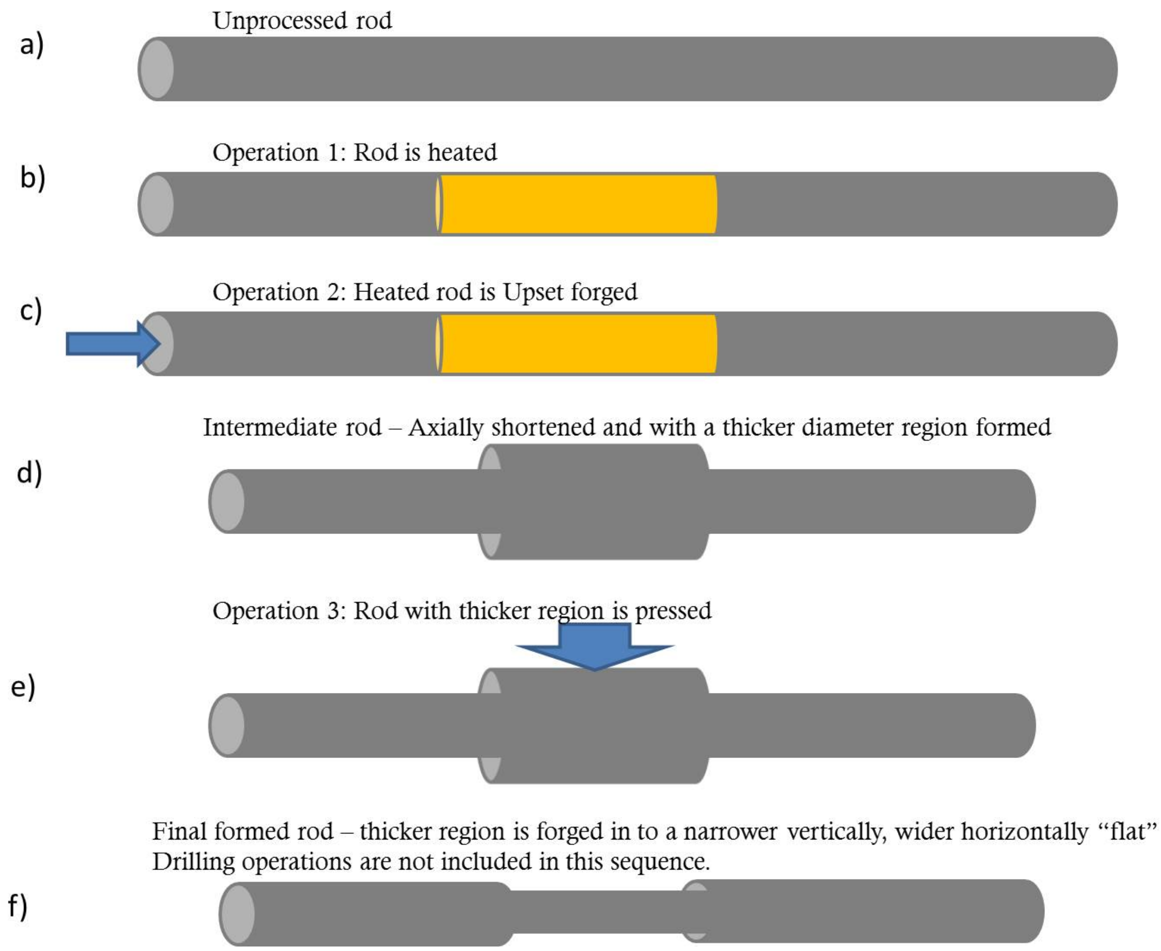

Figure 2: *Various stages of processing operations on the medium carbon boron steel rod, to yield the flattened section fit for mechanical attachment to a conveyor system.*

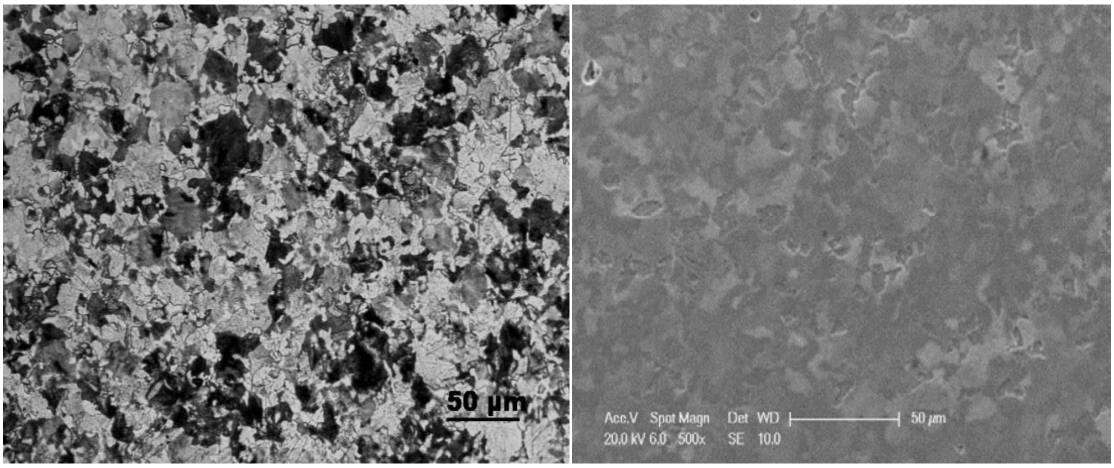

Figure 3a: *As-received microstructure of medium carbon boron steel: (left) - Optical image, (right) - SEM image*

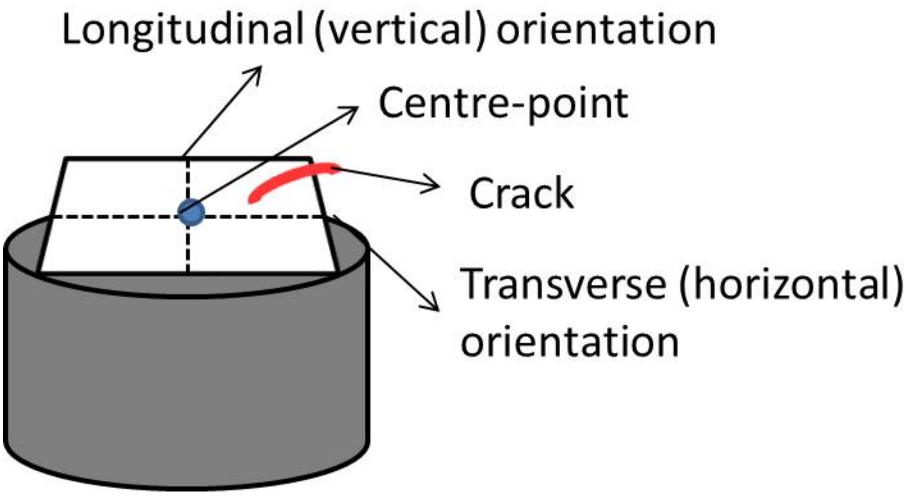

Figure 3b: *Orientations of the directions analysed relative to the crack observed.*

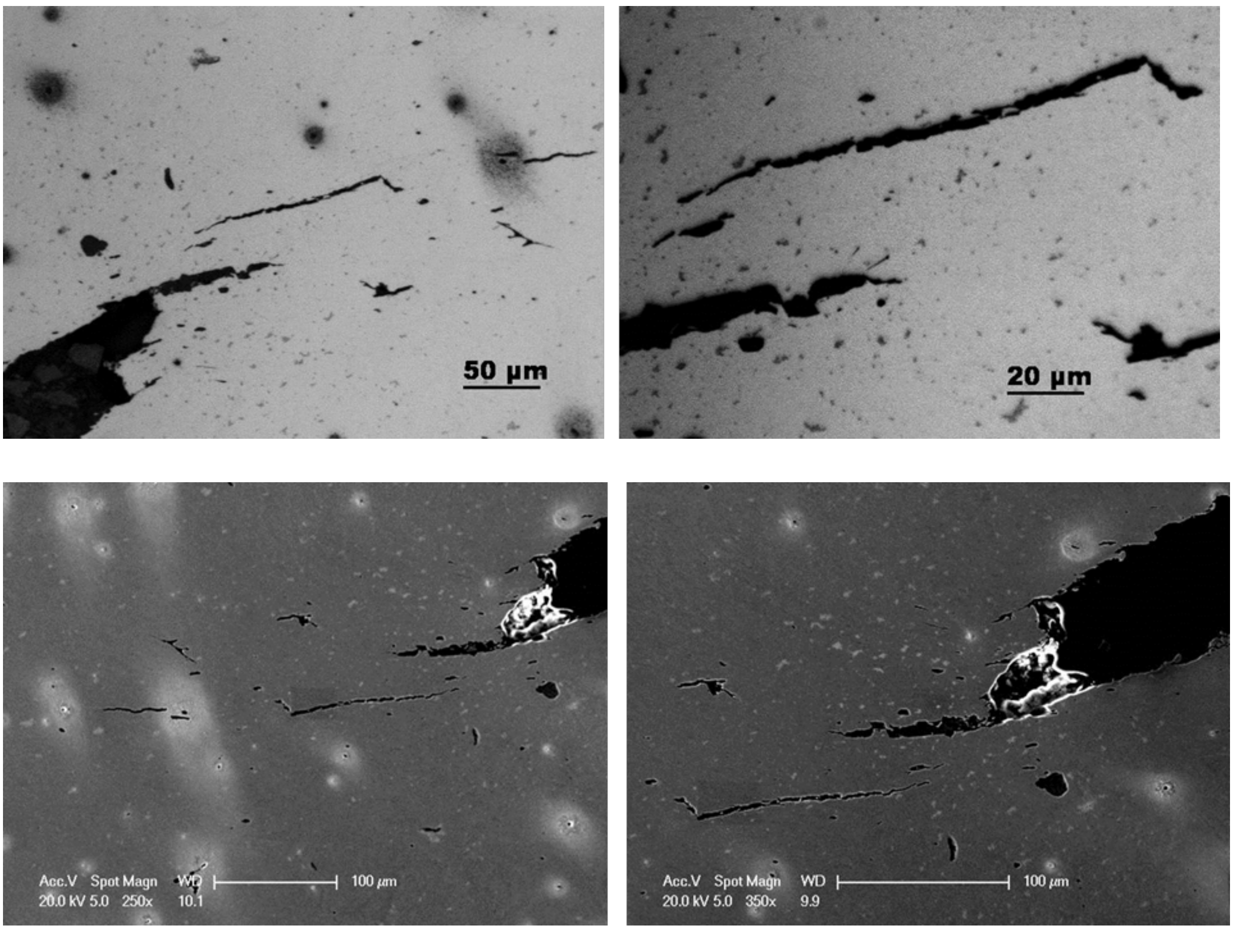

Figure 4: *The optical (upper) and SEM (lower) images shows the intergranular fracture surface of mechanically deformed medium carbon boron steel. Images on the right are at a higher magnification than the left.*

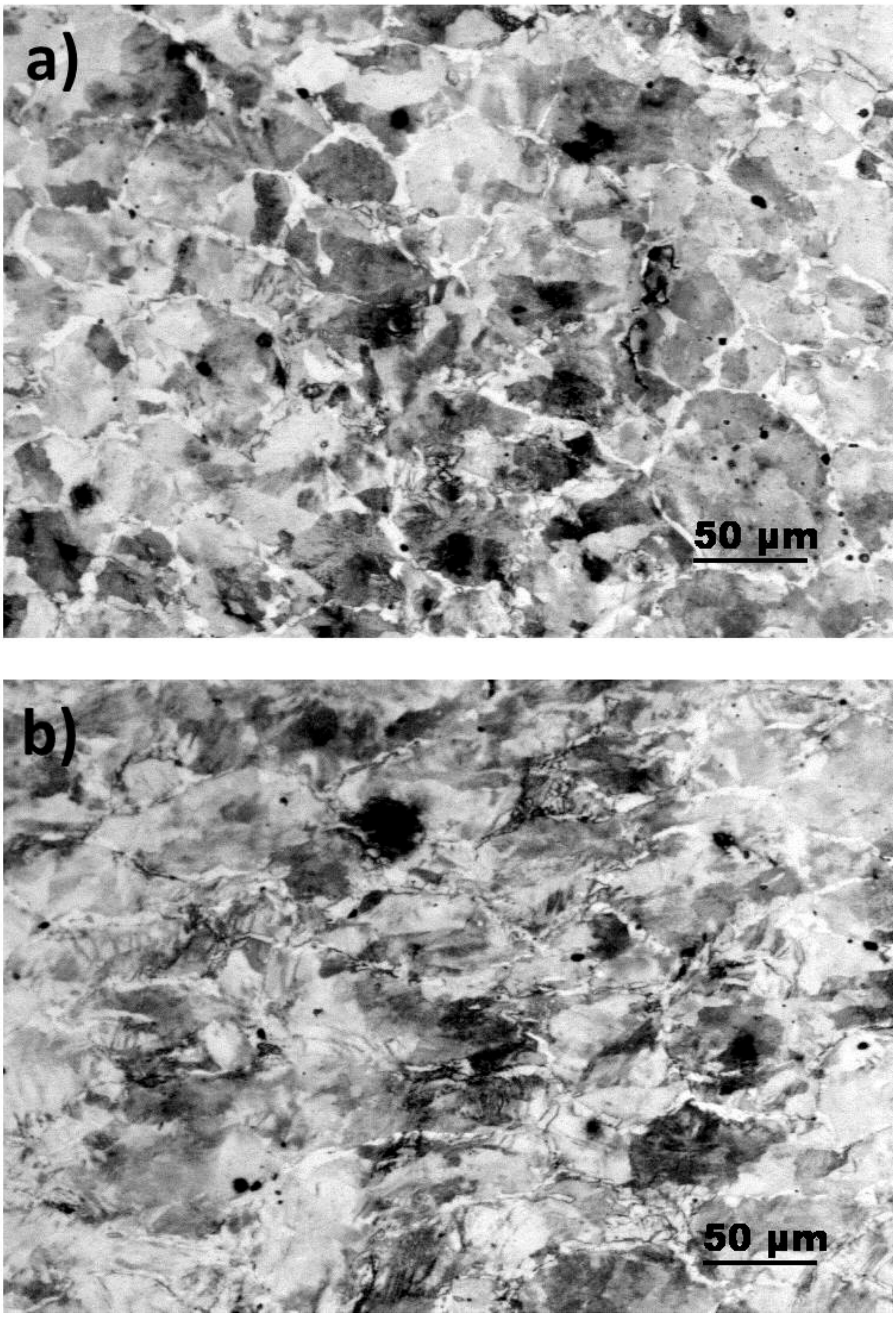

Figure 5: *Optical microscopy images from a location close to the crack-tip; (a) the transverse direction, and (b) the longitudinal direction. Note the appearance of a white network of precipitates found on the austenite grain boundaries of hot worked and air cooled medium carbon boron steel.*

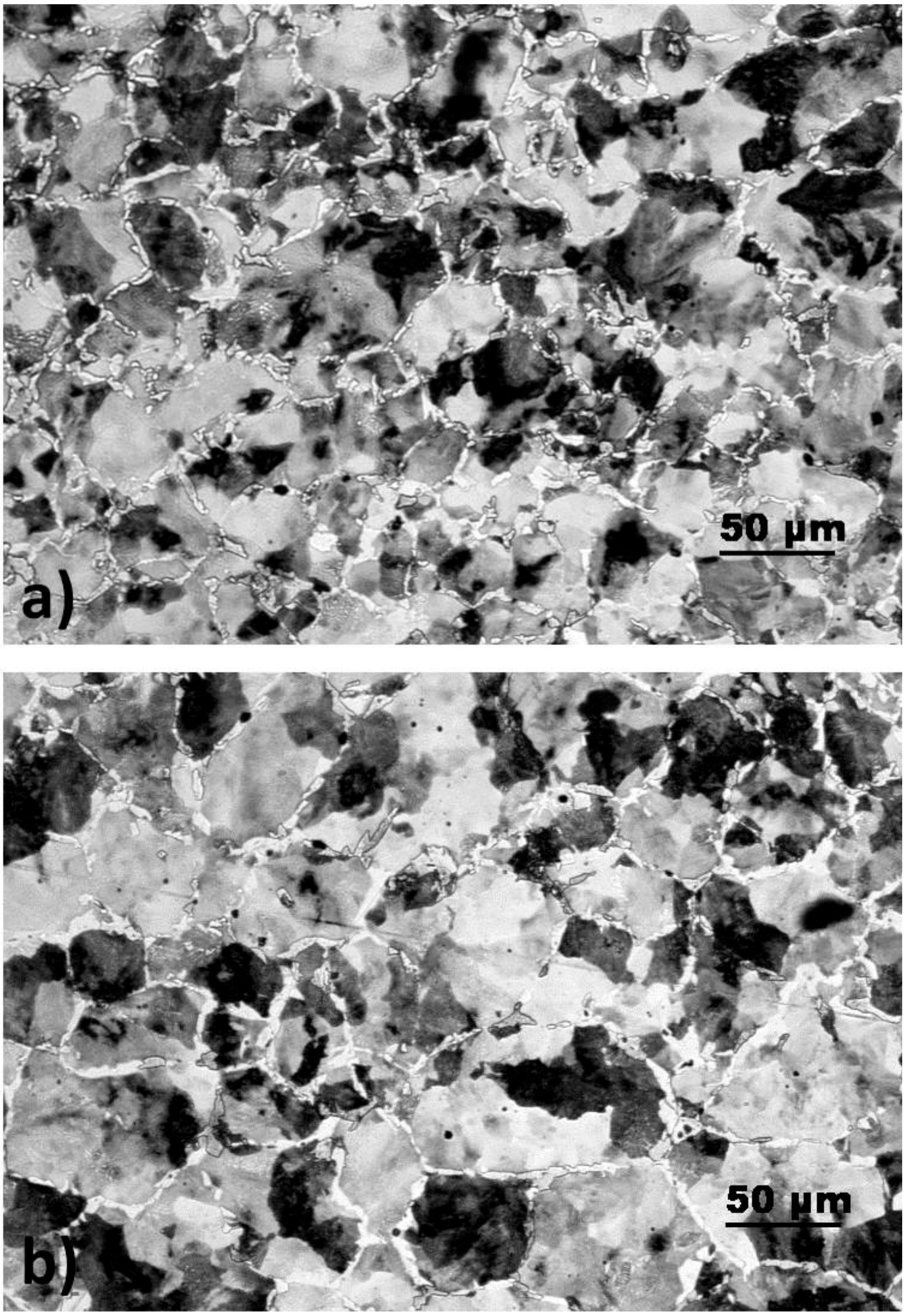

Figure 6: *Optical microscopy images from a) a location close to the crack-tip, and b) a location away from the crack but still in the heated region. Note again the grain boundary network of precipitates in both optical microscopy images, suggesting that the overheating which has caused the precipitation is not just a highly localised feature.*

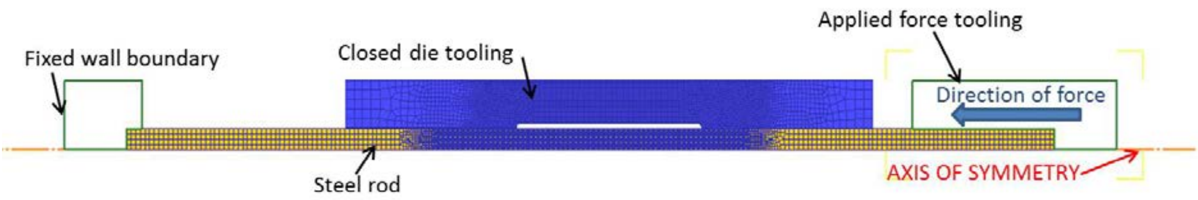

Figure 7a*: Screen-print from FE software showing set-up of the modelling strategy.*

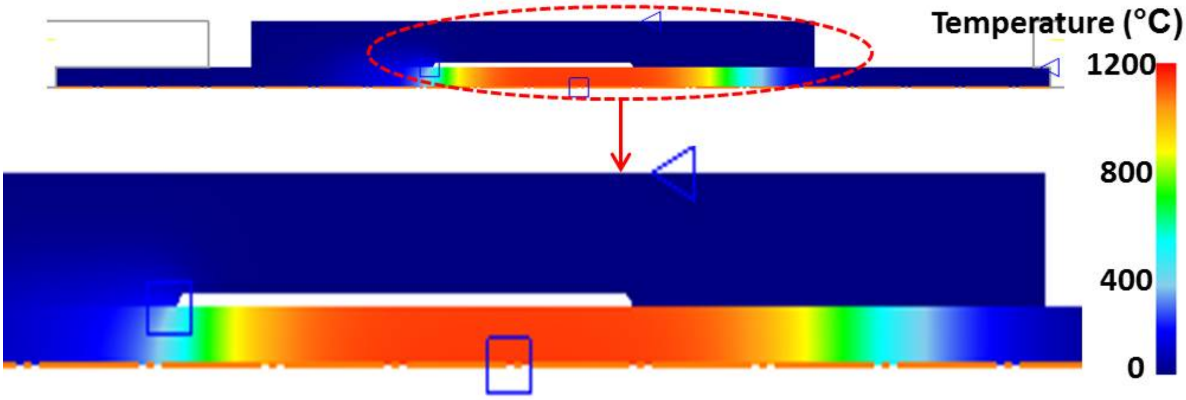

Figure 7b: *Thermal prediction for the rod after the resistive heating operation, and after it has taken approx. 4 seconds to be transferred from the resistive heating unit to the axial forging rig.*

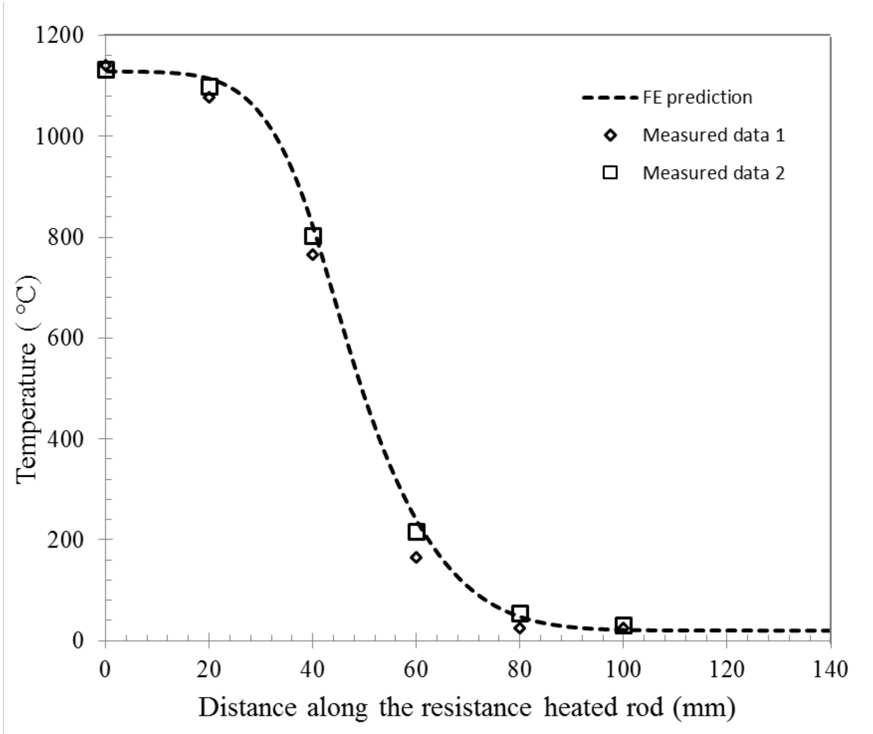

Figure 8: *Thermal profile from the rod after resistive heating, as measured by 20mm spaced temperature readings, and as predicted by FE modelling.*

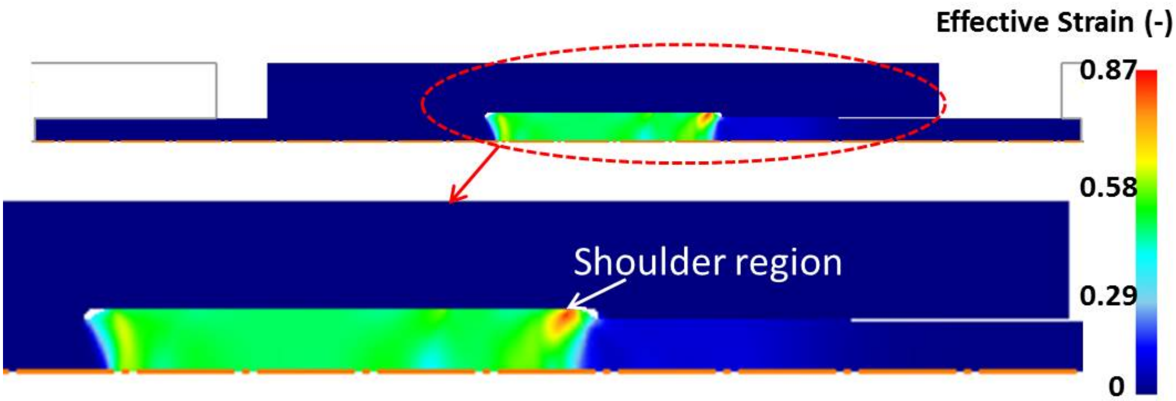

Figure 9a: *Prediction of the effective strain for the rod after it has been subjected to the applied force and undergone axial shortening to form the swelled "bump" region on the axial forging rig.*

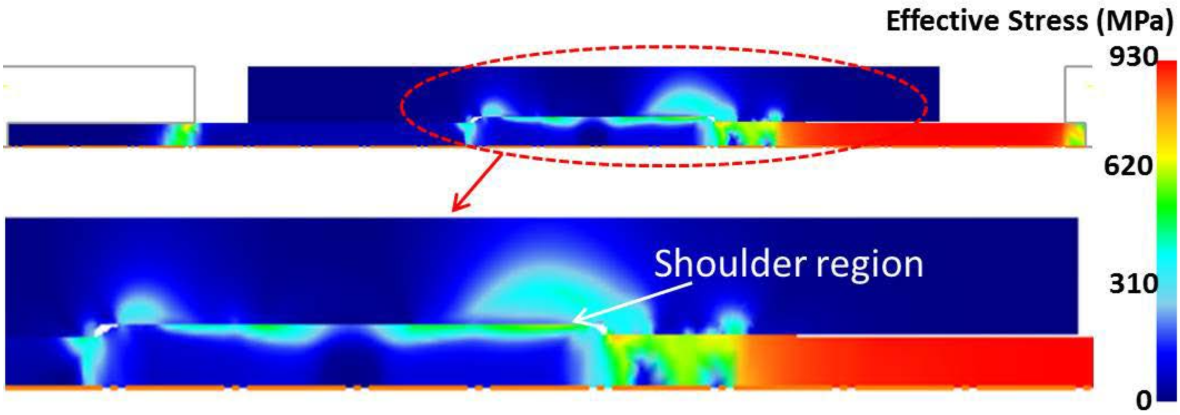

Figure 9b: *Prediction of the effective stress for the rod after it has been subjected to the applied force and undergone axial shortening to form the swelled "bump" region on the axial forging rig.*

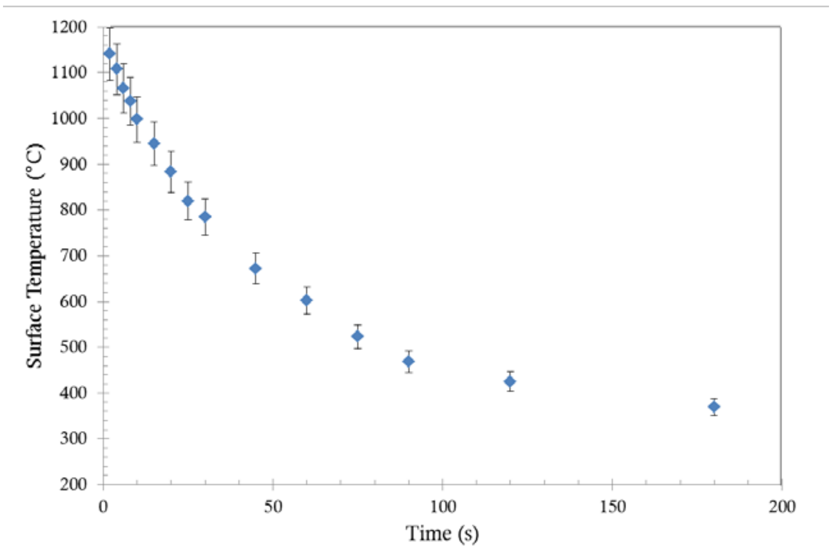

Figure 10: *Thermal history of the heated region of the rod, as measured by infra-red thermometer equipment. The error bars show a +/-5% error margin. This is the maximum error of thermal readings using this equipment.*